



# Er<sup>3+</sup> co-doped Sr<sub>1.956</sub>MgSi<sub>2</sub>O<sub>7</sub>: 0.004Eu<sup>2+</sup>, 0.04Dy<sup>3+</sup> phosphors and enhancement of luminescent properties

Yongfeng Cai<sup>1</sup> · Fengfeng Li<sup>1</sup> · Shiyan Chang<sup>1</sup> · Mingxi Zhang<sup>1</sup> · Zuotao Liu<sup>1</sup> · Yi Shen<sup>1</sup>

Received: 11 December 2017 / Accepted: 16 March 2018 / Published online: 20 March 2018  
© Springer Science+Business Media, LLC, part of Springer Nature 2018

## Abstract

Long afterglow phosphors of Sr<sub>1.956</sub>MgSi<sub>2</sub>O<sub>7</sub>: 0.004Eu<sup>2+</sup>, 0.04Dy<sup>3+</sup> and Sr<sub>1.94</sub>MgSi<sub>2</sub>O<sub>7</sub>: 0.004Eu<sup>2+</sup>, 0.04Dy<sup>3+</sup>, 0.016Er<sup>3+</sup> were successfully synthesized via the sol–gel method. The phase compositions and luminescent properties of the phosphors were analyzed by X-ray diffraction (XRD), fluorescence spectra and decay curves. Compared with the undoped phosphor, the crystallinity of Er<sup>3+</sup> co-doping phosphors is decreased. Luminescence spectra show the main peak of excitation was 274, 356 nm and the main emission peak was 467 nm. Furthermore, Sr<sub>1.94</sub>MgSi<sub>2</sub>O<sub>7</sub>: 0.004Eu<sup>2+</sup>, 0.04Dy<sup>3+</sup>, 0.016Er<sup>3+</sup> show excellent luminescent properties, and its initial luminous intensity increased by 1.4 times than Sr<sub>1.956</sub>MgSi<sub>2</sub>O<sub>7</sub>: 0.004Eu<sup>2+</sup>, 0.04Dy<sup>3+</sup>. The mechanism of Sr<sub>1.94</sub>MgSi<sub>2</sub>O<sub>7</sub>: 0.004Eu<sup>2+</sup>, 0.04Dy<sup>3+</sup>, 0.016Er<sup>3+</sup> enhancement has been discussed.

## 1 Introduction

For more than a decade now, Sr<sub>2</sub>MgSi<sub>2</sub>O<sub>7</sub>: Eu<sup>2+</sup>, Dy<sup>3+</sup> has become a concern for long afterglow phosphors, because of its advantages of luminescent properties [1–8]. In 2005, Alvani et al. [9] successfully prepared Sr<sub>2</sub>MgSi<sub>2</sub>O<sub>7</sub>: Eu<sup>2+</sup>, Dy<sup>3+</sup> via high temperature solid phase method, and discussed the performance and structure of the phosphor in detail. Subsequently, Sr<sub>2</sub>MgSi<sub>2</sub>O<sub>7</sub>: Eu<sup>2+</sup>, Dy<sup>3+</sup> phosphors have been research to preparation methods and doping rare earth elements by many researchers [10–14]. There are two important research aspects: doping rare earth elements and preparation methods.

An important factor of the luminescent to long afterglow phosphors is the doping type and doping concentration of rare earth elements. The luminescence properties of the Sr<sub>2</sub>MgSi<sub>2</sub>O<sub>7</sub> phosphors can be created by doping rare earth ions. The doping type and concentration of rare earth elements are both important factors to phosphors of luminescent properties. Sahu et al. [15] successfully prepared Eu<sup>2+</sup> and Ce<sup>2+</sup> co-doping Sr<sub>2</sub>MgSi<sub>2</sub>O<sub>7</sub> phosphors via high

temperature solid-state reaction. They focus on the effect of the Eu<sup>2+</sup> and Ce<sup>3+</sup> ion radius to decay curve. Wu et al. [16] synthesized the Eu<sup>2+</sup> and Er<sup>3+</sup> co-doping Sr<sub>2</sub>MgSi<sub>2</sub>O<sub>7</sub> phosphors with high temperature solid-state reaction. The results show that the afterglow time in Sr<sub>2</sub>MgSi<sub>2</sub>O<sub>7</sub>: Eu<sup>2+</sup>, Er<sup>3+</sup> is than Sr<sub>2</sub>MgSi<sub>2</sub>O<sub>7</sub>: Eu<sup>2+</sup>, Er<sup>3+</sup> is 1.2 times stronger than that in Sr<sub>2</sub>MgSi<sub>2</sub>O<sub>7</sub>: Eu<sup>2+</sup>. In addition to the two rare earth ions co-doping Sr<sub>2</sub>MgSi<sub>2</sub>O<sub>7</sub> phosphors, Song et al. [17] also attempted that three rare earth ions of Eu<sup>2+</sup>, Dy<sup>3+</sup> and Nd<sup>3+</sup> co-doping Sr<sub>2</sub>MgSi<sub>2</sub>O<sub>7</sub> phosphors.

Although the advantages of high temperature solid-state reaction possesses are less synthesis steps and simple operation, it restricts development to high sintering temperature and unstable luminescent properties. Furusho et al. [18] researched the effect of different sintering temperatures on the luminescent properties. The result indicated the high temperature will influence the structure and phase purity of the Sr<sub>2</sub>MgSi<sub>2</sub>O<sub>7</sub> phosphors. Then, the researchers tried to reduce the synthetic temperature for improving the crystal structure and luminescent properties of the Sr<sub>2</sub>MgSi<sub>2</sub>O<sub>7</sub> phosphors by different preparation methods. Pan et al. [19] successfully synthesized Sr<sub>2</sub>MgSi<sub>2</sub>O<sub>7</sub>: Eu<sup>2+</sup>, Dy<sup>3+</sup> phosphors via co-precipitation method. The solid phase reaction can be completed at 1000 °C, indicating the particle size was uniform and the average particle size was about 1 μm. The Sr<sub>2</sub>MgSi<sub>2</sub>O<sub>7</sub>: Eu<sup>2+</sup>, Dy<sup>3+</sup> phosphors [17] was synthesized via combustion method with average particle size of about 20 nm. Zhang et al. [20] successfully prepared Sr<sub>2</sub>MgSi<sub>2</sub>O<sub>7</sub>: Eu<sup>2+</sup>, Dy<sup>3+</sup> phosphors via sol–gel method. This method has obvious advantages for

✉ Yi Shen  
shenyicyf@126.com

<sup>1</sup> Key Laboratory of Environment Functional Materials of Tangshan City, Hebei Provincial Key Laboratory of Inorganic Nonmetallic Materials, College of Materials Science and Engineering, North China University of Science and Technology, Tangshan 063210, Hebei, China

preparing phosphors, such as a lower synthetic temperature and a fine powder.

In this paper,  $\text{Sr}_{1.956}\text{MgSi}_2\text{O}_7: 0.004\text{Eu}^{2+}, 0.04\text{Dy}^{3+}$  and  $\text{Sr}_{1.94}\text{MgSi}_2\text{O}_7: 0.004\text{Eu}^{2+}, 0.04\text{Dy}^{3+}, 0.016\text{Er}^{3+}$  phosphors were successfully prepared via sol–gel method, and the luminescent properties were improved.  $\text{Er}^{3+}$  ions are doped into  $\text{Sr}_{1.956}\text{MgSi}_2\text{O}_7: 0.004\text{Eu}^{2+}, 0.04\text{Dy}^{3+}$  lattice improve the persistent luminescence due to the formation of exceedingly dense trapping levels situated at appropriate depth. Furthermore, the effects of and  $\text{Er}^{3+}$  on the phase compositions and luminescent properties of  $\text{Sr}_2\text{MgSi}_2\text{O}_7: \text{Eu}^{2+}, \text{Dy}^{3+}$  phosphor were also discussed. The mechanism of  $\text{Sr}_{1.94}\text{MgSi}_2\text{O}_7: 0.004\text{Eu}^{2+}, 0.04\text{Dy}^{3+}, 0.016\text{Er}^{3+}$  enhancement has been discussed.

## 2 Materials and methods

### 2.1 Preparation of the $\text{Sr}_{1.956}\text{MgSi}_2\text{O}_7: 0.004\text{Eu}^{2+}, 0.04\text{Dy}^{3+}$ (SMSSED) and $\text{Sr}_{1.94}\text{MgSi}_2\text{O}_7: 0.004\text{Eu}^{2+}, 0.04\text{Dy}^{3+}, 0.016\text{Er}^{3+}$ (SMSEDE) phosphors

The SMSSED and SMSEDE samples were prepared via sol–gel method. The raw materials  $\text{Sr}(\text{NO}_3)_2$ ,  $\text{Mg}(\text{NO}_3)_2 \cdot 6\text{H}_2\text{O}$  and  $\text{H}_2\text{BO}_3$  were dissolved in  $\text{H}_2\text{O}$  to form solution A, B and C, and the  $\text{H}_3\text{BO}_3$  content was 7.5% of  $\text{Sr}_2\text{MgSi}_2\text{O}_7$ . The  $\text{Dy}_2\text{O}_3$ ,  $\text{Eu}_2\text{O}_3$  and  $\text{Er}_2\text{O}_3$  was dissolved in 3.6M  $\text{HNO}_3$  to form solution D, E and F. The  $\text{Si}(\text{OC}_2\text{H}_5)_4$  was dissolved in absolute ethylalcohol to form solution G. All solutions were fully dissolved under mechanical stirring, respectively. The solutions of B, C, D, E, F were added to solution A under mechanical stirring, affording a mixture solutions. Then, the solution G was slowly added to the mixture and stirred at 70 °C for 2 h. The mixed solution became wet gel after 2 h and the resulting wet gel was dried in an oven at 70 °C for 72 h to obtain a dry gel. Finally, the dry gel was calcined in a muffle furnace at 1100 °C for 3 h. SMSSED was prepared when F was not added.

### 2.2 Characterization

The X-ray diffraction (XRD) patterns were recorded using an X-ray diffractometer (Rigaku D/Max-2500) with Cu K $\alpha$  radiation ( $\lambda = 0.15406$  nm), and diffraction angles ranging from 10° to 80°. The luminescence spectra and decay curves were obtained via a Hitachi F-7000 fluorescence spectrophotometer (Japan) equipped with a 450W Xe lamp as the excitation light-source.

## 3 Results and discussion

Figure 1 shows the X-ray diffraction (XRD) patterns recorded for SMSSED and SESEDE phosphors. It can be seen that all the phosphors are indexed to tetragonal  $\text{Sr}_2\text{MgSi}_2\text{O}_7$

phase with the space group P-421m (No.113) according to JCPDF card no.75-1736. The three peaks (201), (211) and (212) are no offset.  $\text{Er}^{3+}$  co-doping has no significant influence on the structure of the phosphors. However, phosphors of  $\text{Er}^{3+}$  co-doping reduce the intensity of the peak resulting in a decrease in crystallinity.  $\text{Eu}^{2+}, \text{Dy}^{3+}$  and  $\text{Er}^{3+}$  ions are regarded to occupy the  $\text{Sr}^{2+}$  sites in the cell because of the similar covalent radius ( $R_{\text{Sr}} = 1.95$  Å,  $R_{\text{Eu}} = 1.98$  Å,  $R_{\text{Dy}} = 1.92$  Å,  $R_{\text{Er}} = 1.89$  Å) [21, 22].

Figure 2 shows the three-dimensional fluorescence spectra of SMSEDE phosphor. The center of strong emission region appeared at 390 and 467 nm, but the emission region at 390 nm is obviously weaker than 467 nm. This indicates that the best emission wavelength for the  $\text{Eu}^{2+}$  in the host crystal was 467 nm. These two strong emission peaks attributed to the  $4f^65d \rightarrow 4f^7$  transitions of  $\text{Eu}^{2+}$ .  $\text{Sr}^{2+}$  at two different positions in the host lattice can be replaced by  $\text{Eu}^{2+}$  to form two emission centers  $\text{Eu}_1$  and  $\text{Eu}_2$  corresponding to emission at 390 and 467 nm [23]. This because that the  $R_{\text{Sr}} = 1.95$  Å is close to  $R_{\text{Eu}} = 1.98$  Å. The main excitation peaks are 274 and 356 nm, but due to the impact of instrument peak and peak intensity, the experiment will choose the monitoring wavelengths are 356 and 467 nm for emission spectra and excitation spectra, respectively.

Figures 3 and 4 shows that the excitation spectra and emission spectra of the phosphors. This indicates that emission spectra and excitation spectra show that the fluorescence intensity is significantly increased after  $\text{Er}^{3+}$  co-doping. As shown in Fig. 3, under the monitoring wavelength of 467 nm, both of the two phosphors showed two different excitation ranges of 250–330 and 335–450 nm, and the main excitation peak were 274 and 356 nm, indicating that  $\text{Er}^{3+}$  had almost no influence to the excitation peak. The reason why the excitation spectra of SMSEDE is enhanced

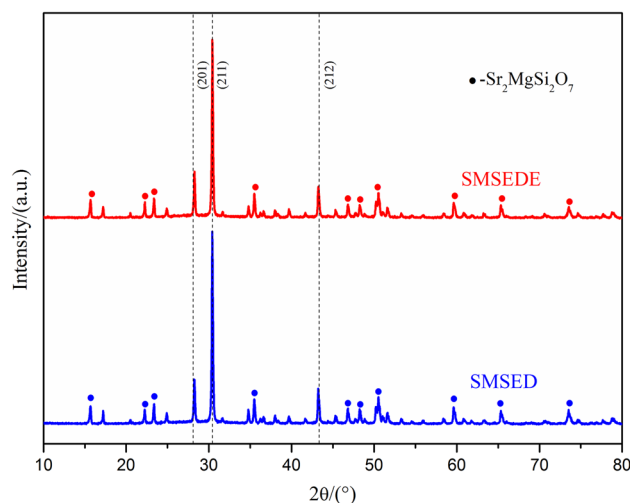


Fig. 1 XRD patterns of SMSSED and SESEDE

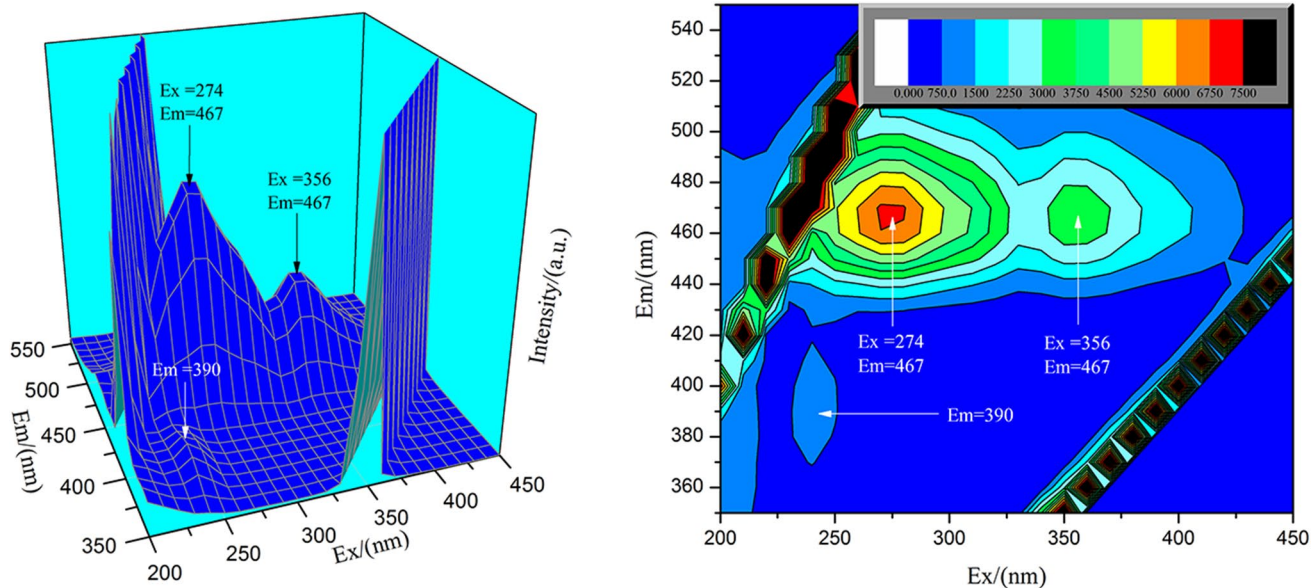


Fig. 2 Three-dimensional fluorescence spectra of the SMSSEDE

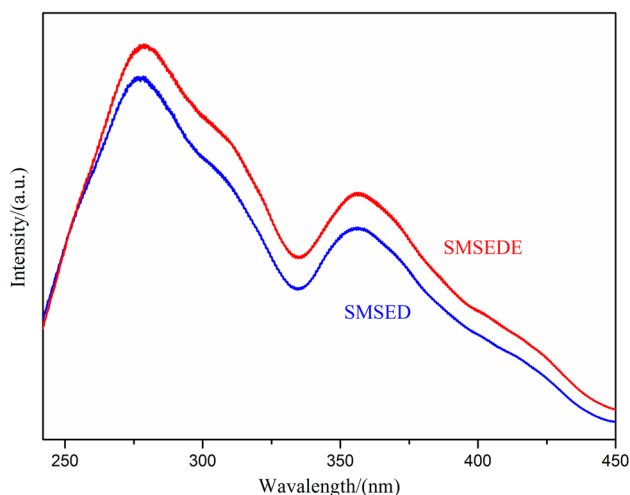


Fig. 3 Excitation spectra of the SMSSED and SMSSEDE

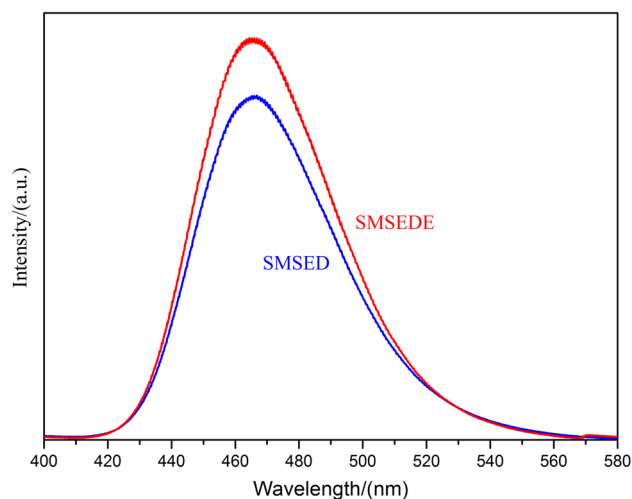


Fig. 4 Emission spectra of the SMSSED and SMSSEDE

is that  $\text{Er}^{3+}$  as a co-doping ion that is  $\text{Eu}^{2+}$  ions makes the distribution of the  $\text{Eu}^{2+}$  ions becomes random and deep throughout the lattice. This result in enhancement of the two excitation peaks at 274 and 356 nm due to the increase of electrons excited by the two characteristic excitation wavelengths. The excitation peak at 274 nm can be attributed to the charge transition of  $\text{Eu}^{2+}-\text{O}^{2-}$ ; the excitation peak at 365 nm can be attributed to the typical  $4f-5d$  emission of  $\text{Eu}^{2+}$  in  $\text{Sr}_2\text{MgSi}_2\text{O}_7$  [24]. As shown in Fig. 4 under the 356 nm excitation wavelength, emission spectra show that the fluorescence intensity is significantly increased after  $\text{Er}^{3+}$  co-doping. The reason why lattice defects are increased after

the introduction of  $\text{Er}^{3+}$  and it acts as an trap to capture and release for electrons or holes [25]. The process affects the recombination of electron-hole pairs to make the intensities of the fluorescence spectra stronger. The emission of 467 nm was assigned to the  $4f^65d^1 \rightarrow 4f^7$  transition of  $\text{Eu}^{2+}$ . The emission peak presented broad-featured, which could be attributed to the stronger crystal field strength of the host material. The characteristic emission peaks of  $\text{Dy}^{3+}$  and  $\text{Er}^{3+}$  are not detected, indicating the  $\text{Eu}^{2+}$  acted an activator, but  $\text{Dy}^{3+}$  and  $\text{Er}^{3+}$  were as co-activators in  $\text{Sr}_2\text{MgSi}_2\text{O}_7$  phosphors. The maximum brightness is achieved when  $\text{Er}^{3+}$  and  $\text{Dy}^{3+}$  auxiliary luminescent particle are incorporated into the

host lattice. The Commission Internationale de l'Eclairage (CIE) chromaticity diagrams [26] of the prepared phosphors are presented in Fig. 5. For all the prepared samples, the CIE chromaticity diagrams fall in the bright blue region.

Figure 6 shows the decay curve of SMSSED and SMSSEDE phosphors. Under the 467 nm excitation wavelength and the 356 nm excitation wavelength, the afterglow decay process usually consists of three sub-decay processes, which can be described by a three-exponential function. The form of the equation is as follows [27]:

$$I = I_0 + I_1 \exp(-t/\tau_1) + I_2 \exp(-t/\tau_2) + I_3 \exp(-t/\tau_3) \quad (1)$$

where  $I$  is phosphorescent intensity,  $I_0, I_1, I_2, I_3$  are the constants,  $t$  is the time,  $\tau_1, \tau_2$  and  $\tau_3$  are time decay constants, respectively. The fitting results of the parameters of  $I_0, I_1, I_2, I_3, \tau_1, \tau_2$  and  $\tau_3$  are listed in Table 1.

The intensity of initial fluorescence ( $I_0$ ) of SMSSEDE is 1.4 times stronger than that in SMSSED, because  $\text{Er}^{3+}$  co-doping could deepen the trap level allowing more free electrons to be trapped. As shown in Fig. 7, the ground state of  $\text{Eu}^{2+}$  transitions to the excited state ( $4f^7 \rightarrow 4f^65d^1$ ) and then some of the electrons enter into the trap during excitation through the lattice. During the afterglow process, electrons are released from the trap to the excited state through thermal excitation and returned to the ground state of the  $\text{Eu}^{2+}$  from the excited state. In other words, the electron transition can be attributed to the  $4f^65d^1 \rightarrow 4f^7$ . Compared with the undoped phosphor, the trap depth of  $\text{Er}^{3+}$  co-doping

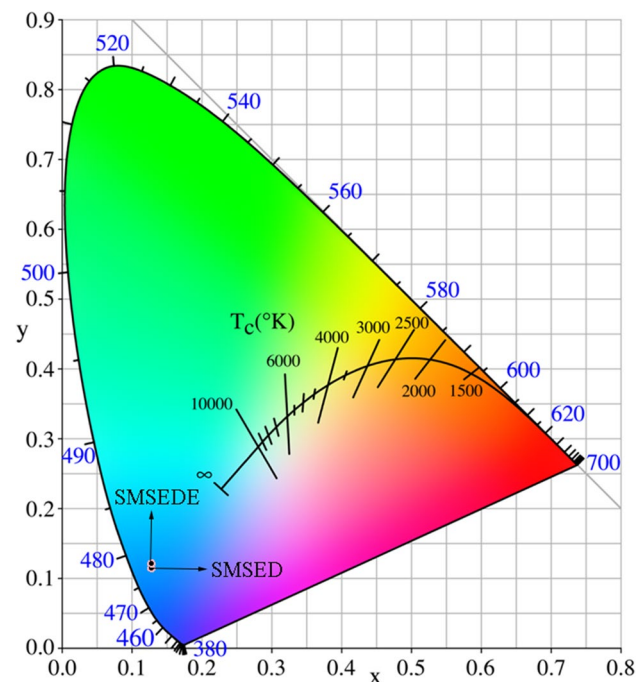


Fig. 5 Chromaticity diagram of SMSSED and SESEDE

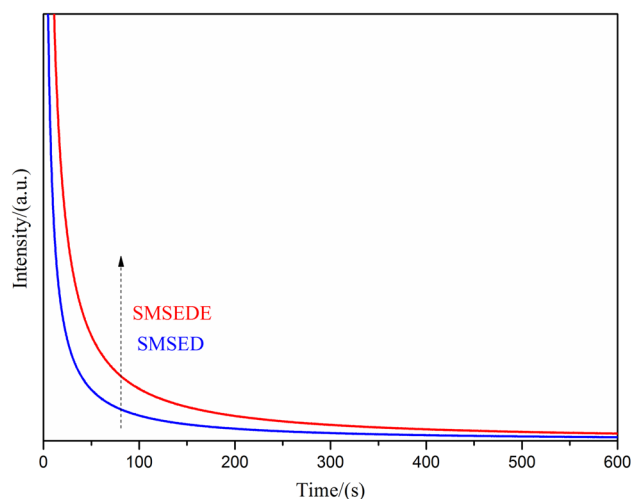


Fig. 6 Decay curves of SMSSED and SMSSEDE. (Color figure online)

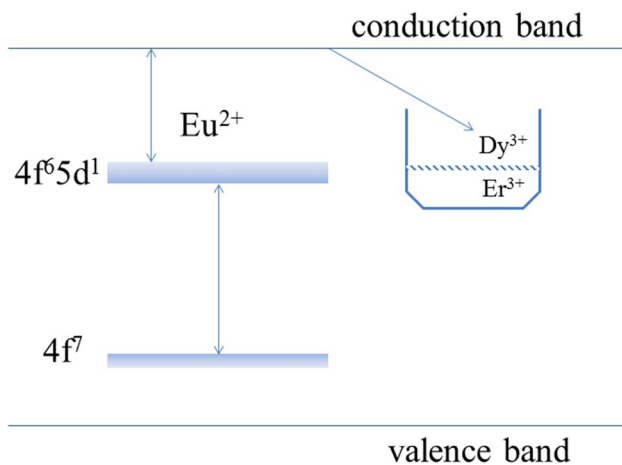
phosphors is increased, so that the fluorescence intensity and afterglow performance will be enhanced.

## 4 Conclusions

In this paper, the  $\text{Sr}_{1.94}\text{MgSi}_2\text{O}_7: 0.004\text{Eu}^{2+}, 0.04\text{Dy}^{3+}, 0.016\text{Er}^{3+}$  phosphor were successfully prepared via sol-gel method. The results show that phosphors of  $\text{Er}^{3+}$  co-doping reduce the intensity of the peak resulting in a decrease in crystallinity. Moreover the luminescent intensity and afterglow performance of  $\text{Er}^{3+}$  co-doping  $\text{Sr}_{1.94}\text{MgSi}_2\text{O}_7: 0.004\text{Eu}^{2+}, 0.04\text{Dy}^{3+}$  phosphors is improved and the  $\text{Sr}_{1.94}\text{MgSi}_2\text{O}_7: 0.004\text{Eu}^{2+}, 0.04\text{Dy}^{3+}, 0.016\text{Er}^{3+}$  phosphor initial luminous intensity increased by 1.4 times than  $\text{Sr}_{1.956}\text{MgSi}_2\text{O}_7: 0.004\text{Eu}^{2+}, 0.04\text{Dy}^{3+}$  phosphor.

**Table 1** Constants of decay curves

Sample	Initial luminance [I (a.u.)]				Decay time [ $\tau$ (s)]		
	$I_0$	$I_1$	$I_2$	$I_3$	$\tau_1$	$\tau_2$	$\tau_3$
SMSSED	0.99	353.41	172.51	31.98	0.15	26.95	172.51
SMSSEDE	1.89	486.68	283.35	54.72	0.22	31.83	283.35

**Fig. 7** The schematic diagram of long-afterglow phosphorescence mechanism of SMSSEDE

**Acknowledgements** This work is supported by the National Science Foundation Project of China (Grant Nos. 51572069 and 51772099).

## References

- H. Furusho, J. Hölsä, T. Laamanen, M. Lastusaari, J. Niittykoski, Y. Okajima, A. Yamamoto, Probing lattice defects in  $\text{Sr}_2\text{MgSi}_2\text{O}_7$ :  $\text{Eu}^{2+}$ ,  $\text{Dy}^{3+}$ . *J. Lumin.* **128**, 881–884 (2008)
- W. Pan, G. Ning, X. Zhang, J. Wang, Y. Lin, J. Ye, Enhanced luminescent properties of long-persistent  $\text{Sr}_2\text{MgSi}_2\text{O}_7$ :  $\text{Eu}^{2+}$ ,  $\text{Dy}^{3+}$  phosphor prepared by the co-precipitation method. *J. Lumin.* **128**, 1975–1979 (2008)
- R. Shrivastava, J. Kaur, Characterisation and mechanoluminescence studies of  $\text{Sr}_2\text{MgSi}_2\text{O}_7$ :  $\text{Eu}^{2+}$ ,  $\text{Dy}^{3+}$ . *J. Radiat. Res. Appl. Sci.* **8**, 201–207 (2015)
- H. Wu, Y. Hu, X. Wang, Investigation of the trap state of  $\text{Sr}_2\text{MgSi}_2\text{O}_7$ :  $\text{Eu}^{2+}$ ,  $\text{Dy}^{3+}$  phosphor and decay process. *Radiat. Meas.* **46**, 591–594 (2011)
- H. Wu, Y. Hu, Y. Wang, C. Fu, Influence on the luminescence properties of the lattice defects in  $\text{Sr}_2\text{MgSi}_2\text{O}_7$ :  $\text{Eu}^{2+}$ , M (M =  $\text{Dy}^{3+}$ ,  $\text{La}^{3+}$ , or  $\text{Na}^{1+}$ ). *J. Alloy. Compd.* **497**, 330–335 (2010)
- H. Homayoni, L. Ma, J. Zhang, S.K. Sahi, L.H. Rashidi, B. Bui, W. Chen, Synthesis and conjugation of  $\text{Sr}_2\text{MgSi}_2\text{O}_7$ :  $\text{Eu}^{2+}$ ,  $\text{Dy}^{3+}$  water soluble afterglow nanoparticles for photodynamic activation. *Photodiagn. Photodyn.* **16**, 90–99 (2016)
- L. He, B. Jia, L. Che, W. Li, W. Sun, Preparation and optical properties of afterglow  $\text{Sr}_2\text{MgSi}_2\text{O}_7$ :  $\text{Eu}^{2+}$ ,  $\text{Dy}^{3+}$  electrospun nanofibers. *J. Lumin.* **172**, 317–322 (2016)
- P. Dorenbos, Mechanism of Persistent Luminescence in  $\text{Eu}^{2+}$  and  $\text{Dy}^{3+}$  codoped aluminate and silicate compounds. *J. Electrochem. Soc.* **152**, H107–H110 (2005)
- A.A.S. Alvani, F. Moztafzadeh, A.A. Sarabi, Preparation and properties of long afterglow in alkaline earth silicate phosphors co-doped by  $\text{Eu}_2\text{O}_3$  and  $\text{Dy}_2\text{O}_3$ . *J. Lumin.* **115**, 147–150 (2005)
- S.H.M. Poort, H.M. Reijnhoudt, H.O.T.V.D. Kuip, G. Blasse, Luminescence of  $\text{Eu}^{2+}$  in silicate host lattices with alkaline earth ions in a row. *J. Alloy. Compd.* **241**, 75–81 (1996)
- O. Hai, H. Jiang, D. Xu, M. Li, The effect of grain surface on the long afterglow properties of  $\text{Sr}_2\text{MgSi}_2\text{O}_7$ :  $\text{Eu}^{2+}$ ,  $\text{Dy}^{3+}$ . *Mater. Res. Bull.* **76**, 358–364 (2016)
- Y. Lin, Z. Tang, Z. Zhang, X. Wang, J. Zhang, Preparation of a new long afterglow blue-emitting  $\text{Sr}_2\text{MgSi}_2\text{O}_7$ -based photoluminescent phosphor. *J. Mater. Sci.* **20**, 1505–1506 (2001)
- H. Wu, Y. Hu, Y. Wang, B. Zeng, Z. Mou, L. Deng Influence on luminescent properties of the  $\text{Sr}_2\text{MgSi}_2\text{O}_7$ :  $\text{Eu}^{2+}$ ,  $\text{Dy}^{3+}$ ,  $\text{Nd}^{3+}$  co-doping. *J. Alloy. Compd.* **486**, 549–553 (2009)
- L. Xiao, J. Zhou, G. Liu, L. Wang, Luminescent properties of  $\text{R}^{+}$  doped  $\text{Sr}_2\text{MgSi}_2\text{O}_7$ :  $\text{Eu}^{2+}$ ,  $\text{Dy}^{3+}$ , ( $\text{R}^{+} = \text{Li}^{+}$ ,  $\text{Ag}^{+}$ ) phosphors. *J. Alloy. Compd.* **712**, 24–29 (2017)
- I.P. Sahu, D.P. Bisen, N. Brahme, R. Sharma, Luminescence properties of  $\text{Eu}^{2+}$ ,  $\text{Dy}^{3+}$ -doped  $\text{Sr}_2\text{MgSi}_2\text{O}_7$  and  $\text{Ca}_2\text{MgSi}_2\text{O}_7$  Phosphors by solid state reaction Method. *Res. Chem. Intermediat.* **41**, 6649–6664 (2015)
- H. Wu, Y. Hu, L. Chen, X. Wang, Enhancement on the afterglow properties of  $\text{Sr}_2\text{MgSi}_2\text{O}_7$ :  $\text{Eu}^{2+}$  by  $\text{Er}^{3+}$  codoping. *Mater. Lett.* **65**, 2676–2679 (2011)
- F. Song, D. Chen, Y. Yuan, Synthesis of  $\text{Sr}_2\text{MgSi}_2\text{O}_7$ :  $\text{Eu}$ ,  $\text{Dy}$  and  $\text{Sr}_2\text{MgSi}_2\text{O}_7$ :  $\text{Eu}$ ,  $\text{Dy}$ ,  $\text{Nd}$  by a modified solid-state reaction and their luminescent properties. *J. Alloy. Compd.* **458**, 564–568 (2008)
- H. Furusho, J. Hölsä, T. Laamanen, M. Lastusaari, J. Niittykoski, Y. Okajima, Probing lattice defects in  $\text{Sr}_2\text{MgSi}_2\text{O}_7$ :  $\text{Eu}^{2+}$ ,  $\text{Dy}^{3+}$ . *J. Lumin.* **128**, 881–884 (2008)
- W. Pan, G. Ning, J. Wang, Y. Lin, J. Ye, Erratum to “Enhanced luminescent properties of long-persistent  $\text{Sr}_2\text{MgSi}_2\text{O}_7$ :  $\text{Eu}^{2+}$ ,  $\text{Dy}^{3+}$  phosphor prepared by the co-precipitation method”. *J. Lumin.* **129**(2009), 584 (2008)
- F. Ye, S. Dong, Z. Tian, S. Zhou, S. Wang, Fabrication and study of properties of the PLA/  $\text{Sr}_2\text{MgSi}_2\text{O}_7$ :  $\text{Eu}^{2+}$ ,  $\text{Dy}^{3+}$  long-persistent luminescence composite thin films. *Opt. Mater.* **40**, 130–135 (2013)
- C.R. Kesavulu, V.B. Sreedhar, C.K. Jayasankar, K. Jang, D.S. Shin, S.S. Yi et al., Structural, thermal and spectroscopic properties of highly  $\text{Er}^{3+}$ -doped novel oxyfluoride glasses for photonic application. *Mater. Res. Bull.* **51**, 336–344 (2014)
- D. Singh, V. Tanwar, A.P. Samantilleke, B. Mari, S. Bhagwan, K.C. Singh, P.S. Kadyan, I. Singh, Synthesis of  $\text{Sr}_{(1-x-y)}\text{Al}_4\text{O}_7$ :  $\text{Eu}_x^{2+}$ ,  $\text{Ln}_y^{3+}$  ( $\text{Ln} = \text{Dy}$ ,  $\text{Y}$ ,  $\text{Pr}$ ) nanophosphors using rapid gel combustion process and their down conversion characteristics. *Electron. Mater. Lett.* **13**, 222 (2017)
- X. Wei, Y. Shen, G. Zuo, L. Hou, Y. Meng, F. Li, Preparation of porous  $\text{Sr}_2\text{MgSi}_2\text{O}_7$ :  $\text{Eu}^{2+}$ ,  $\text{Dy}^{3+}$  energy storage carriers via sol-hydrothermal synthesis. *Ceram. Int.* **41**, 13872–13877 (2015)
- W. Tian, K. Song, F. Zhang, P. Zheng, J. Deng, J. Jiang, J. Xu, H. Qin, Optical spectrum adjustment of yellow–green  $\text{Sr}_{1.99}\text{SiO}_{4-3x/2}\text{N}_x$ :  $0.01\text{Eu}^{2+}$  phosphor powders for near ultraviolet–visible light application. *J. Alloy. Compd.* **638**, 249–253 (2015)

25. F. Li, Z. Li, X. Wang, M. Zhang, Y. Shen, P. Cai, Crystal structure and luminescent property of flaky-shaped  $\text{Sr}_4\text{Al}_{14}\text{O}_{25}$ :  $\text{Eu}^{2+}$ ,  $\text{Dy}^{3+}$  phosphor doped with  $\text{Er}^{3+}$  ions. *J. Alloy. Compd.* **692**, 10–21 (2017)
26. D. Singh, V. Tanwar, A.P. Simantilleke, B. Mari, P.S. Kadyan, I. Singh, Rapid synthesis and enhancement in down conversion emission properties of  $\text{BaAl}_2\text{O}_4$ :  $\text{Eu}^{2+}$ ,  $\text{RE}^{3+}$  ( $\text{RE}^{3+}=\text{Y}$ , Pr) nanophosphors. *J. Mater. Sci.: Mater. Electron.* **27**, 2260–2266 (2016)
27. I. Chen, T. Chen, Sol-gel synthesis and the effect of boron addition on the phosphorescent properties of  $\text{SrAl}_2\text{O}_4$ :  $\text{Eu}^{2+}$ ,  $\text{Dy}^{3+}$  phosphors. *J. Mater. Res.* **16**, 644–651 (2001)